Climate Change Effects on Spatiotemporal Patterns of Hydroclimatological Summer Droughts in Norway

WAI KWOK WONG AND STEIN BELDRING

Norwegian Water Resources and Energy Directorate, Oslo, Norway

TORILL ENGEN-SKAUGEN

Norwegian Meteorological Institute, Oslo, Norway

INGJERD HADDELAND AND HEGE HISDAL

Norwegian Water Resources and Energy Directorate, Oslo, Norway

(Manuscript received 8 July 2010, in final form 20 April 2011)

ABSTRACT

This study examines the impact of climate change on droughts in Norway. A spatially distributed (1×1 km^2) version of the Hydrologiska Byråns Vattenbalansavdelning (HBV) precipitation-runoff model was used to provide hydrological data for the analyses. Downscaled daily temperature and precipitation derived from two atmosphere–ocean general circulation models with two future emission scenarios were applied as input to the HBV model. The differences in hydroclimatological drought characteristics in the summer season between the periods 1961–90 and 2071–2100 were studied. The threshold level method was adopted to select drought events for both present and future climates. Changes in both the duration and spatial extent of precipitation, soil moisture, runoff, and groundwater droughts were identified. Despite small changes in future meteorological drought characteristics, substantial increases in hydrological drought duration and drought affected areas are expected, especially in the southern and northernmost parts of the country. Reduced summer precipitation is a major factor that affects changes in drought characteristics in the south while temperature increases play a more dominant role for the rest of the country.

1. Introduction

Droughts are complex natural hazards that, to a varying degree, affect some parts of the world every year. Even in Norway with its abundant freshwater resources, severe and prolonged water deficit periods have caused major problems in recent years. Low lake and groundwater levels threatened water supply in northern and western Norway in the winter of 2009/10, and electricity prices rose to unprecedented high levels as a result of the extreme low reservoir storages. Similar situations occurred in 2006, 2002/03, and 1995/96. Trend studies indicate that summer droughts in southern Norway have become more severe (Wilson et al. 2010), and according to the latest Intergovernmental Panel on Climate Change (IPCC) Fourth Assessment Report (Solomon et al. 2007), most atmosphere–ocean general circulation models (AOGCMs) project an increased dryness of summer soil moisture across large areas of the northern middle and high latitudes.

Summer and winter droughts can be distinguished based on their driving hydrological processes. Summer droughts are caused by natural climate variability leading to precipitation deficits over some periods of time (meteorological droughts). The lack of precipitation propagates through the hydrological cycle, which combined with high evapotranspiration losses, can cause soil moisture deficiencies and subsequently streamflow and groundwater depletion (Tallaksen and van Lanen 2004). Winter droughts refer to low levels of streamflow and groundwater storage due to precipitation being stored as snow and ice (Hisdal et al. 2001). Soil moisture droughts are commonly referred to as agricultural droughts. Here, for simplicity, they are

Corresponding author address: Wai Kwok Wong, Norwegian Water Resources and Energy Directorate, NVE, P.O. Box 5091, Majorstuen, Oslo N-0301, Norway.
E-mail: wkw@nve.no

DOI: 10.1175/2011JHM1357.1

together with runoff and groundwater droughts termed hydrological droughts. In this paper, summer droughts defined as precipitation, soil moisture, runoff, or groundwater below a predefined threshold level are examined. This definition is applicable to both meteorological and hydrological time series, and is of direct relevance to the water industry when investigating environmental demands on river systems.

Climate change has the potential to alter hydrological conditions and these changes could have a large adverse effect on the availability of the water resources. Few studies have examined climate change impacts on future droughts. A study by Calanca (2007) stated that the frequency of soil moisture droughts will increase in summer in the Alpine region in Europe. Blenkinsop and Fowler (2007) used six regional climate models (RegCMs) to study the impact of climate change on the British Isles and discovered an increase in short term summer precipitation droughts. At the continental scale, Lehner et al. (2006) suggested that the recurrence of today's 100-year streamflow drought will be less frequent in Scandinavia because of a large projected increase in the average discharge. Sheffield and Wood (2008) analyzed soil moisture results from eight AOGCMs and three emission scenarios. They found relatively small changes in the frequency of short term soil moisture droughts (4–6 months) in northern Europe toward the end of the century but significant changes in the droughts' spatial extent. Feyen and Dankers (2009) assessed the effect of climate change on streamflow drought in Europe by the end of this century. Their results, presented in the form of maps, revealed that streamflow droughts in Norway in nonfrost season will become more severe and persistent. With the exception of the conclusions in Lehner et al. (2006), these studies all indicate more severe summer droughts in the future. However, the conclusions in these studies are based on coarse spatial resolution data and are therefore considered insufficient for the development of climate change adaptation strategies. The lack of accuracy in climate change projections at the regional and local scales makes it difficult for the planners and water managers to take directed action to respond to climate change (Ludwig et al. 2009).

Droughts are regional in nature and usually cover large areas, and should, hence, be studied within a regional context (Hisdal and Tallaksen 2003). An assessment of regional drought characteristics, such as the spatial extent, provides critical information for different water-based activities including water supply and hydropower production, and should be included in strategic short and long term plans for sound water resource management. In Hisdal and Tallaksen (2003) and Tallaksen et al. (2009), time series of hydroclimatological variables were simulated in a grid over a region to determine the area affected by drought. In this study a similar approach is employed. A spatially distributed, gridded (1×1 km^2) version of the Hydrologiska Byråns Vattenbalansavdelning (HBV) precipitation-runoff model developed at the Swedish Meteorological and Hydrological Institute is forced with downscaled precipitation and temperature data to generate daily time series of different hydrological components (Beldring et al. 2003).

The main objective of this study is to compare the effect of climate change on hydroclimatological droughts in Norway for the periods 1961–90 (referred to as present climate) and 2071–2100 (future climate). To assess the impact of temperature and precipitation changes on hydrological droughts, the spatial variability and relative changes in drought duration based on two emission scenarios and two AOGCMs are examined. Future changes in the average drought affected areas for the whole country are examined. Norway spans a large area from north to south; the same weather pattern may give very different hydrological responses in different regions. Consequently, a more detailed study of the changes in the spatial extent of droughts is confined to the Glomma River basin—the largest river basin in Norway.

2. Data

a. Study area

Norway covers an area of 325 000 km^2 in northern Europe (Fig. 1). The mean annual precipitation ranges from approximately 300 to 3500 mm. The highest precipitation amounts are found in western and northern Norway. The average annual runoff is estimated to be 1140 mm—that is, about 25% of the precipitation is returned to the atmosphere as evapotranspiration (Beldring et al. 2002). The hydrological regime in mountainous and inland areas of Norway is characterized by a low winter runoff due to the storage of winter precipitation as snow. In western Norway, especially in the coastal areas, late autumn is the wettest period of the year and low flows can occur both in summer and winter. Precipitation is usually in the form of snow during the period November to March, with snowmelt occurring from April to June. Norwegian aquifers generally have a limited storage capacity consisting mainly of small precipitation-fed till deposits (low permeable glacier debris). In the coastal regions, both soil moisture and groundwater are normally at their lowest level in summer because of a lack of precipitation and high evapotranspiration. For inland regions, soil moisture and groundwater usually have two minima: one in summer and one in winter. The winter minimum is a result of precipitation being stored as snow, effectively stopping the recharge. The general variability of groundwater recharge and depletion are typically

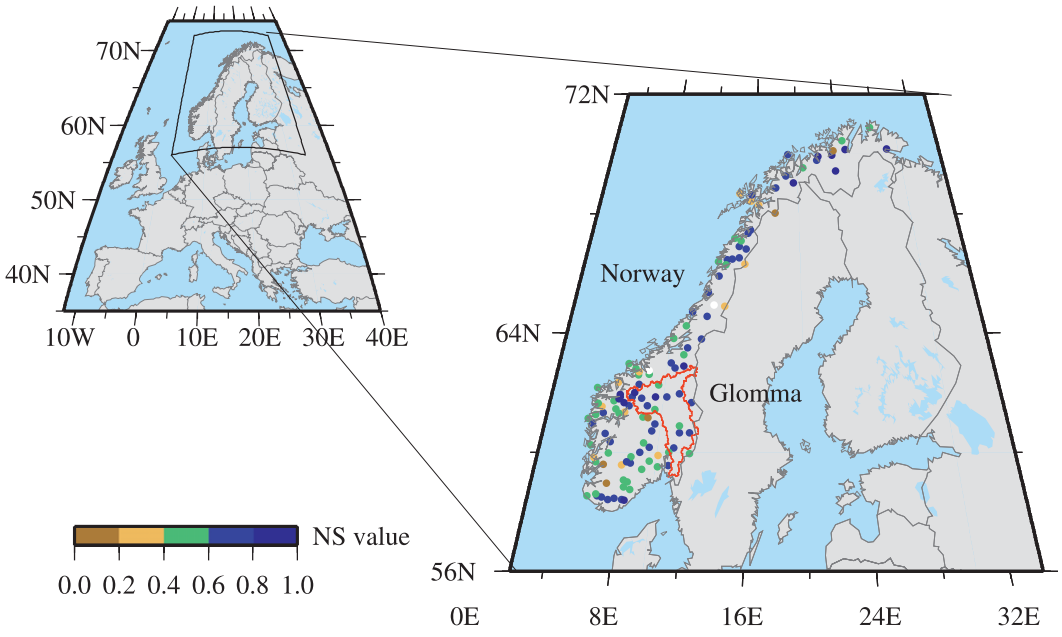

FIG. 1. Location of the study area. The Glomma River basin is outlined in red. The colored dots represent the location and Nash–Sutcliffe value of the 121 basins used for calibration of the HBV model.

larger than in coastal regions. The Glomma River basin is located in southeastern Norway (Fig. 1), covering an area of 42 000 km^2. Mean annual precipitation and runoff is about 800 and 530 mm, respectively. The annual runoff distribution is heavily influenced by snow accumulation and melt.

b. Climate data

A time slice approach was adopted including two 30-year periods representing present (control period: 1961–90) and projected (2071–2100) conditions. Two general circulation models (GCMs) were used: the AOGCM ECHAM4/Ocean Isopycnal Model (OPYC3) developed at the Max Planck Institute for Meteorology (MPI; Roeckner et al. 1999) in Germany and the Hadley Centre Atmospheric Model, version 3, high resolution (HadAM3H) coupled with boundary conditions from the third climate configuration of the Met Office Unified Model (HadCM3) both developed at the Met Office's Hadley Centre (HAD; Gordon et al. 2000) in the United Kingdom. MPI has a good reproduction of the Norwegian present climate with dominant westerly winds. HAD has a different atmospheric circulation pattern also typical in Norway, more dominated by south-easterly winds. Together these two models cover a relatively large variability in potential future change. HAD was run with emission scenarios A2 and B2 (HAD/A2 and HAD/B2) from the Special Report on Emissions Scenarios (SRES). MPI was only run with B2 (MPI/B2) (Nakićenović and Swart 2000). HAD and MPI were dynamically downscaled using the HIRHAM RegCM with a spatial resolution of 0.5° (~55 × 55 km^2) by the Norwegian Meteorological Institute (met.no) (Haugen and Iversen 2008). To examine the representativeness of these projections among the other existing ones for Norway, they were compared to an ensemble of 72 climate projections (Hanssen-Bauer et al. 2009). The HAD/A2 and MPI/B2 projections of the summer mean temperature (June–August) are slightly above and HAD/B2 slightly below the mean of the ensemble. The HAD/A2 summer precipitation is below the 10th percentile of an ensemble of projections, whereas the HAD/B2 is similar to the ensemble mean. The MPI/B2 projection is between HAD/A2 and B2.

The resulting RegCM datasets are still too coarse for input into the hydrological model. Furthermore, the precipitation amount and number of wet days are often overestimated (Frei et al. 2003). Postprocessing of RegCM data is, thus, necessary to make the data locally applicable. An empirical adjustment method was used (Engen-Skaugen 2007). The purpose of this method is to reproduce the statistical properties of the observed meteorological conditions for the control period. The adjustment procedure requires the mean and standard deviation for each calendar month. These values were derived from the daily gridded (1 × 1 km^2) datasets of precipitation and temperature fields for the period 1961–90 developed by met.no (Tveito et al. 2005).

3. Model and method

a. The hydrological model

Water balance modeling for the land surface of Norway was performed using a spatially distributed version of the HBV model (Beldring et al. 2003). The model calculates the water balance for 1×1 km^2 grid cells characterized by their elevation and land use. The model was run at a daily time step, using precipitation and air temperature data as input. It includes subgrid scale accumulation and ablation of snow, interception storage, subgrid scale distribution of soil moisture storage, evapotranspiration, groundwater storage and runoff response, lake evaporation, and glacier mass balance.

The algorithms of the model are described by Bergström (1995). In short, potential evapotranspiration is a function of air temperature and seasonally varying vegetation characteristics. The structure of the HBV model has been designed with the aim of providing realistic simulations of soil moisture and groundwater storage and their impact on runoff response. The HBV model simulates the spatial distribution of soil moisture content in the unsaturated zone and the volume of groundwater storage for each computational element of the model. There is no flow of soil moisture or groundwater between grid cells in the HBV model. However, because of the combination of shallow surface deposits and hard, crystalline bedrock in Norway, this rarely occurs at the spatial scale of 1×1 km^2 used in this study.

Melting of glacier ice starts when the snow covering the glacier surface has melted. Glacier ice melts at a faster rate than snow because of its lower albedo. Snow storage present at the glacier surface at the end of the ablation season is converted to ice before the accumulation season begins. The HBV model applied in this study does not simulate soil ice. Although frozen soil may hinder infiltration of water and thereby generate overland flow that contributes to a rapid increase of streamflow, the discontinuous nature of soil frost in the Nordic countries means that runoff generation is generally not influenced by this phenomenon (Vehviläinen and Motovilov 1989).

Because of the absence of directly measured catchment characteristics, natural variability, and nonlinearity of the processes involved, calibration is necessary to adjust the model parameters to improve the model's ability to reproduce the observed hydrological data. A regional set of parameters for each land use class were determined using a multicriteria calibration strategy, where the residuals between simulated and observed daily streamflow from 121 Norwegian basins (see Fig. 1) located in areas with different hydrological regimes and landscape characteristics were considered simultaneously. This calibration procedure rests on the hypothesis that model elements with identical landscape characteristics have similar hydrological behavior (Gottschalk et al. 2001). The period 1991–2000 was chosen as the calibration period because of its large variability in hydrological processes ensuring proper calibration of all the model components. Model results were generally good. Fifty percent of the results have the Nash–Sutcliffe efficiency criterion exceeding 0.6 and 30% over 0.7 (Fig. 1). Eighty percent of the results have an absolute volume error less than 5%. The performance of the model has also been verified previously (see, e.g., Bergström and Sandberg 1983; Lindström et al. 1997; Colleuille et al. 2008). Colleuille et al. (2008) examined the performance of the model for several water balance components, including snow storage, soil moisture in the unsaturated zone, groundwater storage, and runoff using observed data on these processes from all regions in Norway. Runoff and evapotranspiration fluxes determined by the HBV model are usually realistic when observed precipitation, temperature, and streamflow data are available for model calibration.

b. Definition of summer season and threshold level

Model simulations produced gridded daily time series of soil moisture, runoff, and groundwater. These datasets, together with the downscaled precipitation data, constituted the basis of this study. Although the HBV model was run continuously for the whole study period, only the results from the summer season were analyzed. Based on an evaluation of the mean daily temperature in the present climate, it was found that the period 15 May–15 October generally has mean temperatures above 0°C across the whole country. This period was therefore chosen as the summer season for both the control and projection periods. This season definition implies that a drought can develop and last for a maximum of 154 days and that multiyear droughts do not occur. Using a fixed summer season simplifies the comparisons of the temporal and spatial changes in drought characteristics, while avoiding the risk of a false conclusion that increased drought duration in the future is the result of a longer summer season. A changing climate with increasing temperatures will, however, prolong the summer season, and this should be considered when interpreting the results.

To minimize the effect of minor droughts, a 7-day moving-average procedure as recommended by Fleig et al. (2006) was applied prior to further analyses. Within each grid cell, drought events were selected from daily time series of precipitation, soil moisture, runoff, and groundwater by applying the threshold level method. The threshold selection depends on the hydrological regime under study and the type of analysis to be carried out. Hisdal et al. (2004) concluded that based on exceedance frequencies, thresholds between the 90th and 70th percentiles

are reasonable choices for perennial rivers. After analyzing the exceedance frequency of the relevant variables from the control period, the 80th percentile (the value exceeded 80% of the time) was found to be an appropriate threshold. This percentile, based on the control period, was consistently applied to all the variables in both the control and projection periods. When comparing future changes in drought characteristics, this choice ensures that the threshold is a constant absolute value and consequently the relative change in drought duration can be studied. This has the advantage of simplicity and allows direct comparison of the changes in meteorological and hydrological drought characteristics.

c. Definition of drought characteristics

The drought characteristics developed by Tallaksen et al. (2009) were used in the Glomma River basin. To reduce the local scale variability and focus on the larger droughts, a minimum area criterion of 20% was adopted as proposed by Tallaksen et al. (2009). A drought event is identified if at least 20% of the basin grid cells are below their respective thresholds. For each time step, each individual grid cell was examined to determine if it was below its threshold. Following Tallaksen et al. (2009), an indicator function $I_{i,t}$ was used:

$$I_{i,t} = \begin{cases} 1 & \text{for} \quad X_{i,t} < \tau_i \\ 0 & \text{for} \quad X_{i,t} \geq \tau_i \end{cases}, \tag{1}$$

where $X_{i,t}$ is a variable for grid cell i and time step t and τ_i is the threshold level for grid cell i.

The total number of grid cells found to be in drought was calculated, and K_t validated whether the minimum 20% criterion was fulfilled at time step t:

$$K_t = \begin{cases} 1 & \text{for} \quad \sum_{i=1}^{M} I_{i,t} > 0.2M \\ 0 & \text{for} \quad \sum_{i=1}^{M} I_{i,t} \leq 0.2M \end{cases}, \tag{2}$$

where M is the number of grid cells within the Glomma River basin (41 549). Drought duration for each drought event j, D_{Gj}, could be obtained accordingly:

$$D_{Gj} = \sum_{t=1}^{L_{Gj}} K_t, \tag{3}$$

where L_{Gj} is the number of consecutive time steps in drought j under which the 20% criterion is met.

For each identified drought event, the average and maximum areas covered by a drought were derived. The average area in drought event j, $\overline{A}_j$, is defined as

$$\overline{A}_j = \frac{\sum_{t=1}^{L_{Gj}} \sum_{i=1}^{M} I_{i,t} \frac{1}{M}}{L_{Gj}}, \tag{4}$$

where $j = 1, 2, \ldots$, is the number of drought events in the study period.

The maximum area covered by a drought event j, $A_{\max_j}$, is

$$A_{\max j} = \max\left(\sum_{i=1}^{M} I_{i,t} \frac{1}{M}; \quad t = 1, 2, \ldots, L_{G_j} \right). \tag{5}$$

The future changes in drought characteristics in the Glomma River basin can be found by comparing D_G, $\overline{A}$, and $A_{\max}$ between the control and projection periods. However, when changes are considered at the country scale, such event-based drought characteristics become inapplicable because they typically lead to droughts lasting for the whole summer season because of the highly heterogeneous hydrological conditions in Norway. This study therefore examined drought characteristics based on individual grid cells. The duration of a drought event j for grid cell i, $D_{i,j}$, is defined as

$$D_{i,j} = \sum_{t=1}^{L_{i,j}} I_{i,t}, \tag{6}$$

where $L_{i,j}$ is the number of consecutive time steps t in drought j for grid cell i.

For each grid cell two drought characteristics were derived: average and maximum drought duration. Average drought duration for grid cell i, $\overline{D}_i$, is the mean duration of all the drought events that occur in a study period:

$$\overline{D}_i = \frac{1}{N_i} \sum_{j=1}^{N_i} D_{i,j}, \tag{7}$$

where N_i is the number of drought events in the study period for grid cell i. Maximum drought duration for grid cell i, $\overline{D}_{\max_i}$, is defined as the mean duration of the 10 longest drought events:

$$\overline{D}_{\max i} = \frac{1}{10} \sum \max_{10}(D_{i,j}; \quad j = 1, 2, \ldots, N_i), \tag{8}$$

where $\max_{10}$ is the 10 longest drought events of the period.

In addition, the average area of Norway affected by drought, $\overline{A}_{\text{NOR}}$, is defined as

$$\overline{A}_{\text{NOR}} = \sum_{t=1}^{T} \sum_{i=1}^{W} I_{i,t} \frac{1}{W}, \tag{9}$$

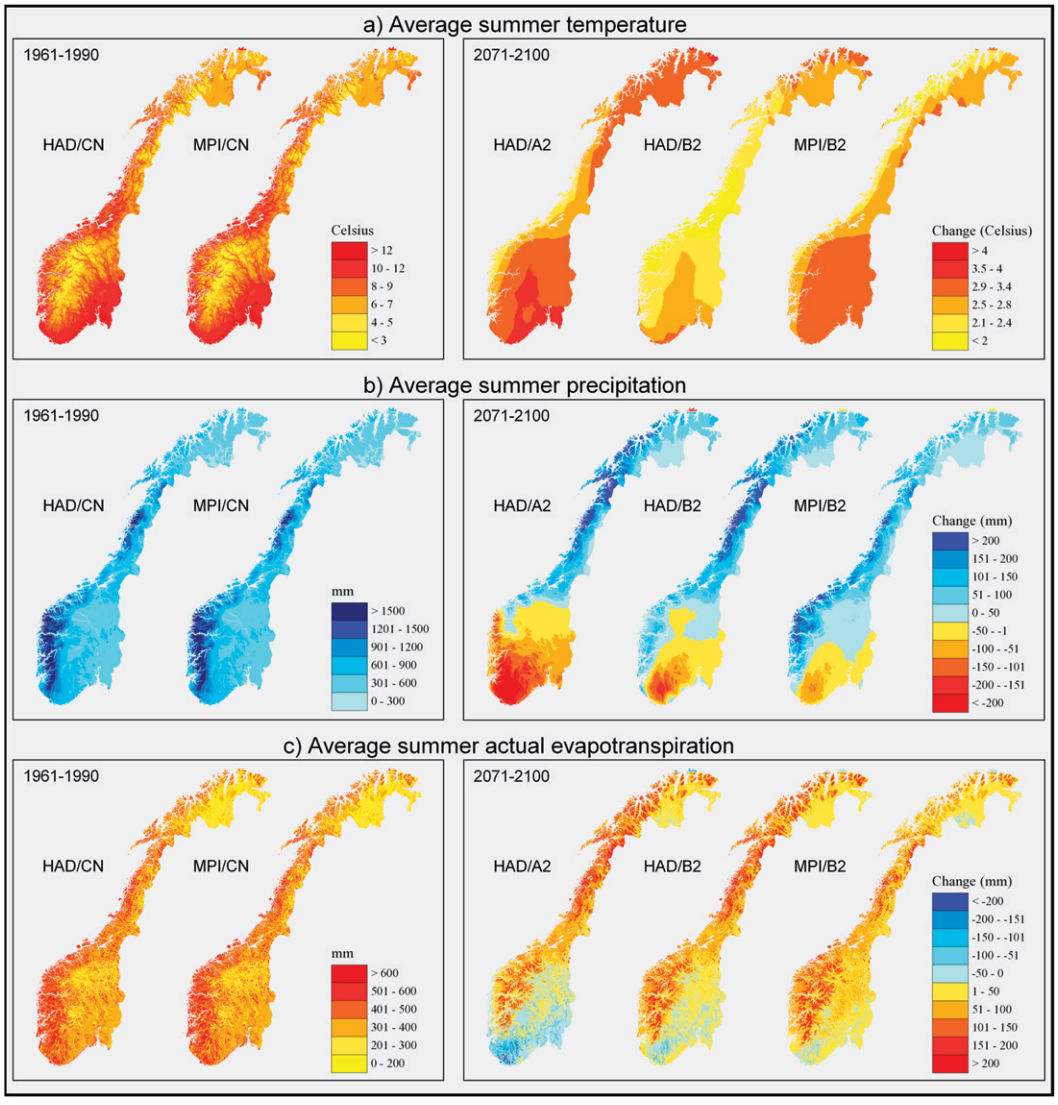

FIG. 2. (a) Average summer temperature (1961–90) and projected future changes (2071–2100), (b) average summer precipitation (1961–90) and projected future changes (2071–2100), and (c) average summer actual evapotranspiration (1961–90) and projected future changes (2071–2100).

where W is the number of grid cells covering the land surface of Norway (324 565) and T is the number of summer days in the study period (4620).

The spatial pattern of changes in drought duration in Norway can be revealed by systematically plotting $\overline{D}_i$ and $\overline{D}_{\max_i}$, where $i = 1, 2, \ldots, W$. To examine whether the changes in drought characteristics, $\overline{D}$ and $\overline{D}_{\max}$, between the control and projection periods were statistically significant, t tests with 5% significance level were applied (Larsen and Marx 1986).

4. Results

Both HAD and MPI produce insignificant differences in mean summer temperature and precipitation in the period 1961–90 (Fig. 2). All projections predict a warmer summer season (15 May–15 October) for the whole country with a temperature increase of 1°–4°C (Fig. 2a). The largest increase can be expected in southeastern and northern Norway, with the smallest increase along the west coast. Generally HAD/A2 projects the largest temperature changes, especially in southernmost Norway with an increase of about 4°C. The regional mean temperature pattern of MPI/B2 is similar to that of HAD/A2, but with a smaller temperature increase in southernmost and northern Norway. HAD/B2 depicts a smaller increase in mean temperatures, generally 1°–1.5°C lower than the other two projections.

According to all projections, mid- and northern Norway will experience an increase in future summer precipitation from 100 to over 200 mm (Fig. 2b). In southernmost and western Norway, regional differences between the projections are greatest. While MPI/B2 predicts up to a 200-mm increase in precipitation in southwestern Norway, HAD/A2 projects a 50–200-mm reduction. Moreover, MPI/B2 projects only a slight decline in summer precipitation in the southernmost part of the country, but this reduction is significantly larger in HAD/A2 (up to 200 mm and above) and is expected to affect the whole of southern Norway. The largest variability in changes across the country can be observed in HAD/A2. The precipitation projection of HAD/B2 is intermediate to HAD/A2 and MPI/B2.

Average summer actual evapotranspiration will increase because of increased summer temperatures, except in regions where a considerable reduction is predicted in summer precipitation (Fig. 2c). This is most pronounced for HAD/A2 in southernmost Norway.

a. Comparison of drought characteristics between observed and downscaled control data

To study the impact of the downscaling method on changes in drought characteristics, the HBV model was forced with ''observed'' gridded precipitation and temperature data for the period 1961–90 (Tveito et al. 2005). The 80th percentiles of the observed data were used as threshold levels and drought characteristics ($\overline{D}$ and $\overline{D}_{\max}$) were derived. They were compared with drought characteristics based on downscaled control data (HAD and MPI) applying the observed threshold values. The significance test (*t* test with 5% significance level) showed that for most of the country (78%–98%) the average drought duration derived from the downscaled control data was not significantly different from the observed drought characteristics. For maximum drought duration, the test results indicated a higher discrepancy. The nonsignificance percentage was about 60 for the hydrological variables and 71 (MPI) and 83 (HAD) for precipitation.

b. Changes in drought characteristics: National scale

The average and maximum drought durations [Eqs. (7)–(8)] for precipitation, soil moisture, runoff, and groundwater were calculated for both the control and projection periods for each grid cell. For each time period and variable, the cumulative distribution functions (CDFs) of $\overline{D}$ and $\overline{D}_{\max}$ were derived. In Fig. 3 the CDF of each variable as a function of duration is shown. The CDFs represent the nationwide variability of drought duration for each variable of interest.

The simulations based on the downscaled temperature and precipitation from HAD and MPI perform similarly in the control period (CN), indicating comparable average drought duration variability (Fig. 3). For maximum drought duration, the differences between HAD/CN and MPI/CN are slightly greater. Results indicate that meteorological droughts are short, lasting only a few days on average, up to a maximum of 25 days for the mean of the 10 most severe drought events. Hydrological droughts last longer. For soil moisture, the average drought duration is 20–30 days for most of the country, with a maximum drought duration of 40–70 days. Similar durations are found for runoff and groundwater, although their variability across the country is larger.

For the projection period, results reveal little change in average meteorological drought duration over the country [panel (i) of Fig. 3a], but the 10 longest meteorological droughts are expected to last longer—up to 35 days [panel (ii) of Fig. 3a]. Generally the hydrological droughts in Norway [i.e., soil moisture (Fig. 3b), runoff (Fig. 3c), and groundwater droughts (Fig. 3d)] are expected to become more persistent. This is observed both for average and maximum drought durations. Average runoff and groundwater drought duration for most of the country ranges from 20 to 140 days. For soil moisture droughts, the corresponding average duration is 20–80 days. Maximum hydrological drought duration shows similar results to the average duration with an even larger increase in the future climates [panel (ii) of Figs. 3b–d]. The season-long persistence of runoff and particularly groundwater droughts is projected to become more widespread, to around 5% and 20% of Norway, respectively [panel (ii) of Figs. 3c,d]. For most of the country, the maximum drought duration ranges from 40 to 154 days, the longest possible duration based on the definition of the summer season. Maximum soil moisture drought duration varies between 50 and 120 days [panel (ii) of Fig. 3b].

Although droughts in Norway will generally last longer in the future, considerable geographical differences in these changes are anticipated. The spatial distributions of the significant changes in average and maximum drought duration are presented in Figs. 4 and 5. The darker red the color, the larger the increase in drought duration; the darker blue the color the larger the decrease, while green symbolizes no significant change. The change in the average meteorological drought duration for the country as a whole is fewer than 3 days (Fig. 4a). The largest increase in average drought duration in soil moisture (Fig. 4b), runoff (Fig. 4c), and groundwater (Fig. 4d) is expected in southern Norway, with an increase of 31–60 days. Northernmost Norway is also likely to experience longer hydrological droughts (16–30 days). Another feature worth noting is the significant increase in the average groundwater

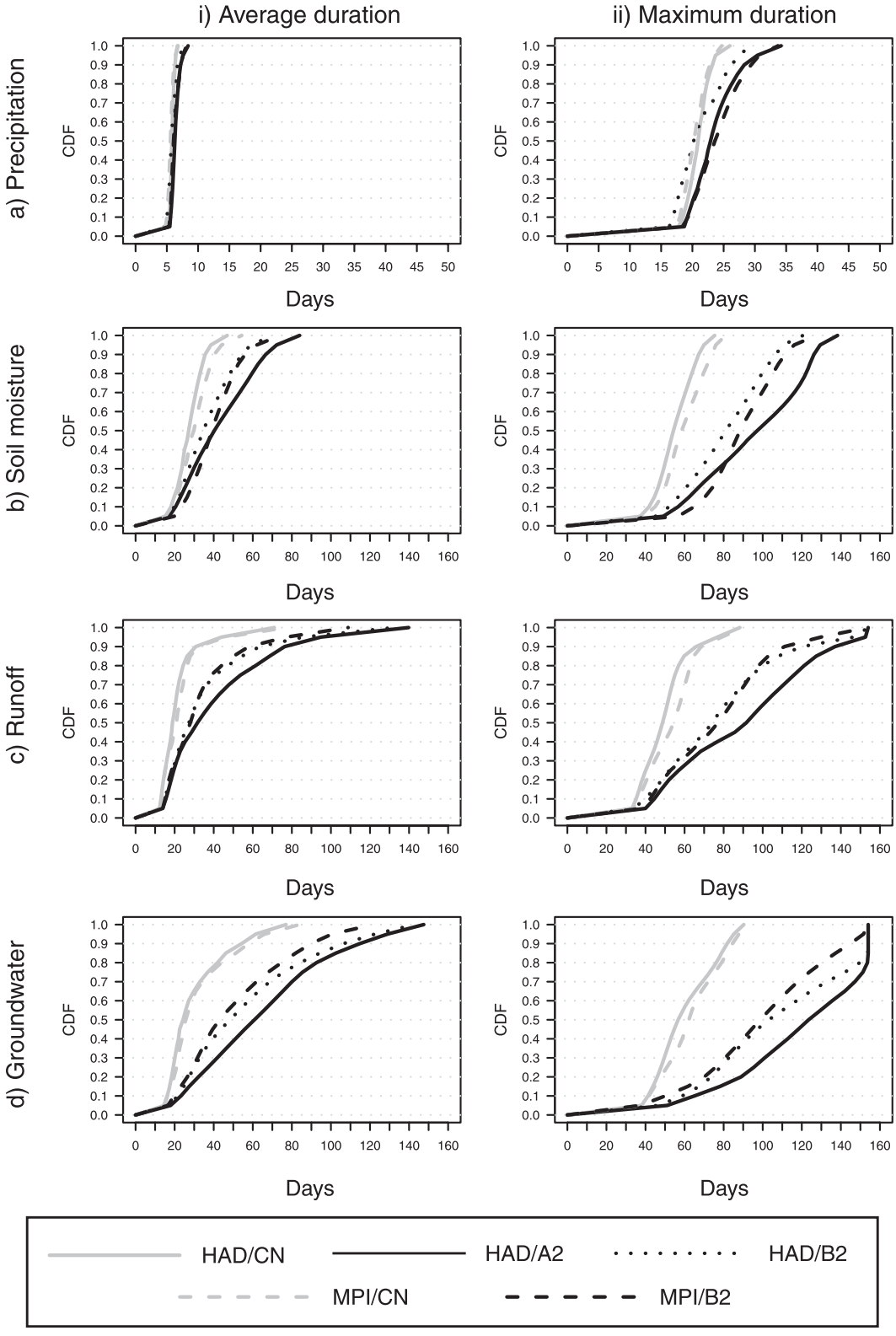

FIG. 3. The cumulative distribution function of drought duration characteristics for Norway for (a) precipitation, (b) soil moisture, (c) runoff, and (d) groundwater. The solid and dashed gray lines represent HAD/CN and MPI/CN, respectively, for the control period (1961–90). The solid, dotted, and dashed black lines represent HAD/A2, HAD/B2, and MPI/B2 for the projection period (2071–2100).

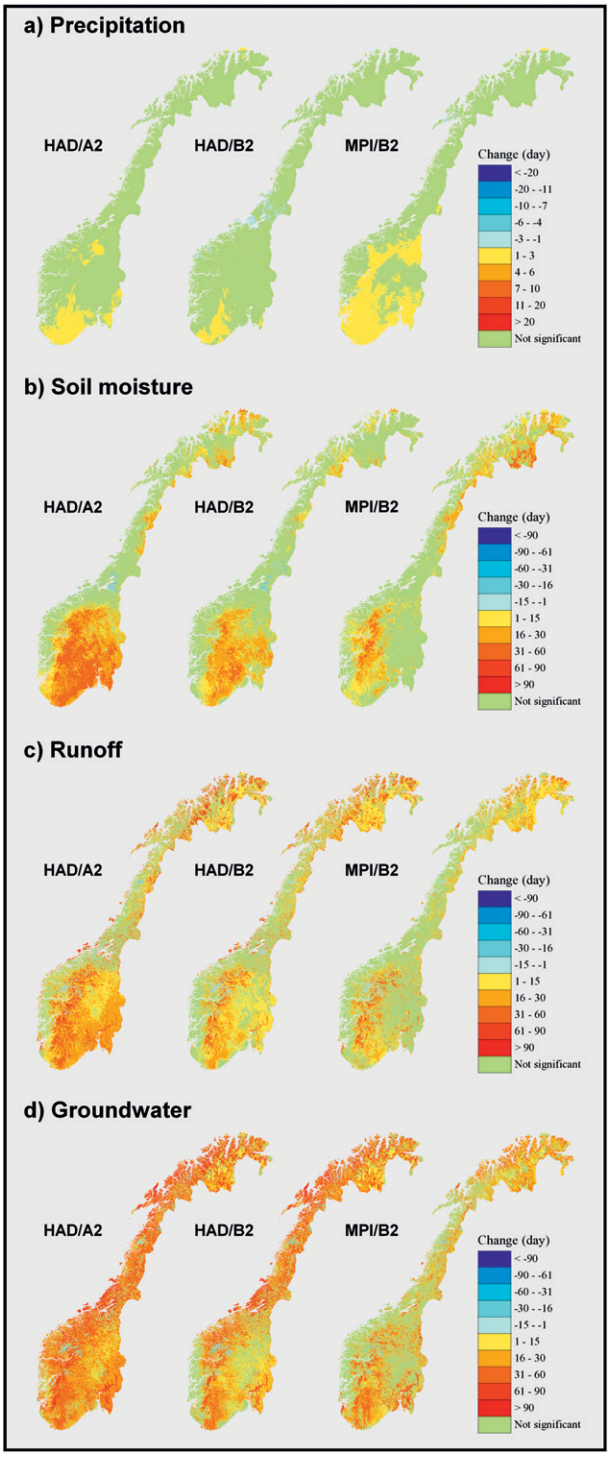

FIG. 4. Significant changes (t tests with 5% significance level) in average drought duration from the control period (1961–90) to the projection period (2071–2010) for (a) precipitation, (b) soil moisture, (c) runoff, and (d) groundwater, respectively.

drought duration (Fig. 4d). Practically the whole country is expected to experience groundwater droughts with substantially longer durations, ranging from 16 to 60 days. The only exception is areas dominated by glaciers where a reduction of 16–30 days is projected. These are indicated in Fig. 4d as blue areas. A similar reduction in drought duration for areas dominated by glaciers can also be seen for runoff (Fig. 4c), though smaller in magnitude.

The spatial changes in maximum drought duration are shown in Fig. 5. All projections show that the 10 longest meteorological droughts are expected to last at least 11–20 days longer in southernmost Norway (Fig. 5a). HAD/B2 predicts a shortened maximum drought duration of up to 10 days for western, mid-, and the northernmost part of Norway. However, these reductions are almost absent in the other projections. HAD/A2 suggests a 3-month-longer duration for the longest hydrological droughts in large parts of southern Norway (Figs. 5b–d). The other two projections indicate that the most severe droughts will last up to 2 months longer. The increase in maximum drought duration in groundwater is considerably larger than the other hydrological variables (Fig. 5d). The most severe groundwater droughts will last 2–3 months longer in most parts of the country.

The threshold level adopted (80th percentile) implies that the average area of Norway affected by drought ($\overline{A}_{\mathrm{NOR}}$) in the control period is 20%. Depending on the projections, the average area in drought increases to 38%–55% for groundwater. The same increase applies to runoff (35%–44%) and soil moisture (40%–49%). However, the analyses show only a minor increase for precipitation (21%–24%). HAD/A2 consistently predicts the largest increase.

c. *Changes in drought characteristics: Basin scale*

Only MPI/B2 shows a slight increase in average meteorological drought duration ($\overline{D}$) up to 3 days in the northeastern and southern parts of the Glomma River basin (Fig. 4a). However, almost no significant increase in average soil moisture drought duration in the basin can be found for MPI/B2, whereas HAD/A2 shows a significant increase for the whole basin (Fig. 4b). Similar features can also be observed for runoff and groundwater droughts (Figs. 4c,d) with HAD/A2 having the largest significant increases in average duration. The results are the same when maximum drought duration ($\overline{D}_{\mathrm{max}}$) is considered (Figs. 5c,d). Applying the 20% minimum threshold area criterion prior to the derivation of the drought characteristics [D_G, $\overline{A}$, and A_{max}; Eqs. (3)–(5)], the results indicate droughts with longer duration and larger area coverage. However, these drought characteristics are averaged over the Glomma River basin. The

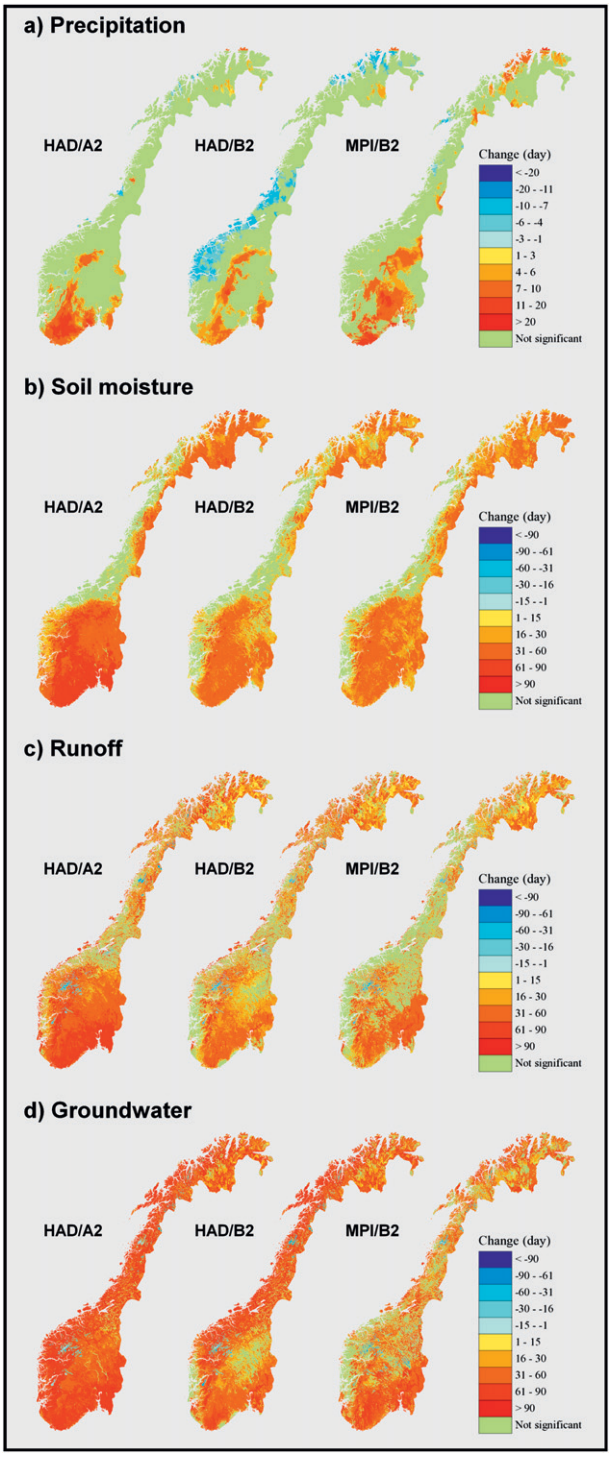

FIG. 5. Same as Fig. 4, but for maximum drought duration.

CDFs shown in Fig. 6 therefore describe the variability of the droughts in the basin, rather than individual grid cells.

Approximately 90% of meteorological droughts in the Glomma River basin during the control period last fewer than 15 days [panel (i) of Fig. 6a]. The average spatial extent of drought in some cases reaches 100% [panel (ii) of Fig. 6a]. Regarding maximum spatial extent, 30% of the meteorological droughts cover the whole basin completely [panel (iii) of Fig. 6a]. Generally, future climate projections show insignificant increases in the characteristics of meteorological drought. Half of the soil moisture droughts last fewer than 25 days in the control period [panel (i) of Fig. 6b]. As much as 70% of the runoff droughts and 60%–70% of the groundwater droughts last fewer than 25 days [panel (i) of Figs. 6c,d]. In the future, 50%–60% of the hydrological droughts are expected to have a duration longer than 40 days [panel (i) of Figs. 6b–d]. Half of the hydrological droughts cover an average area of 30%–80% in the control period, but the average areal coverage for half of future hydrological droughts increases to 60%–90% for soil moisture, 45%–90% for runoff, and 40%–80% for groundwater [panel (ii) of Figs. 6b–d]. The results also indicate a doubling of the maximum spatial extent from 20%–50% to over 90% for half of the soil moisture droughts. Increases in maximum coverage are also expected for runoff and groundwater droughts, though less significant, ranging from 20%–40% in the control period to 20%–60% in the future period.

The increase in both the duration and areal extent are most pronounced for medium-sized droughts. The average areal coverage during a drought is generally much higher for meteorological droughts than the hydrological droughts. Groundwater droughts often have the longest duration, but the average area affected is the smallest [panel (ii) of Fig. 6d].

5. Discussion

a. Mechanisms of drought

Increases in summer temperature will increase potential evapotranspiration due to increased atmospheric demand. If precipitation does not increase sufficiently to compensate for increased evapotranspiration, drier conditions will result—that is, increased soil moisture deficit, reduced runoff, and groundwater storage. A decrease in summer precipitation will further reduce soil moisture, which might in turn decrease groundwater recharge and runoff generation. The HAD/A2 predicts the largest increase in drought duration (Figs. 4–5)—a consequence of this scenario projecting the largest overall increase in mean summer temperature for the whole country (Fig. 2a) and the largest reduction in summer precipitation in southern Norway (Fig. 2b).

When future hydrological droughts are considered, it is clear that an increase in temperature plays a more dominant role than an increase in precipitation because the actual evapotranspiration increases (Fig. 2c). Despite the projected increase in summer precipitation and negligible

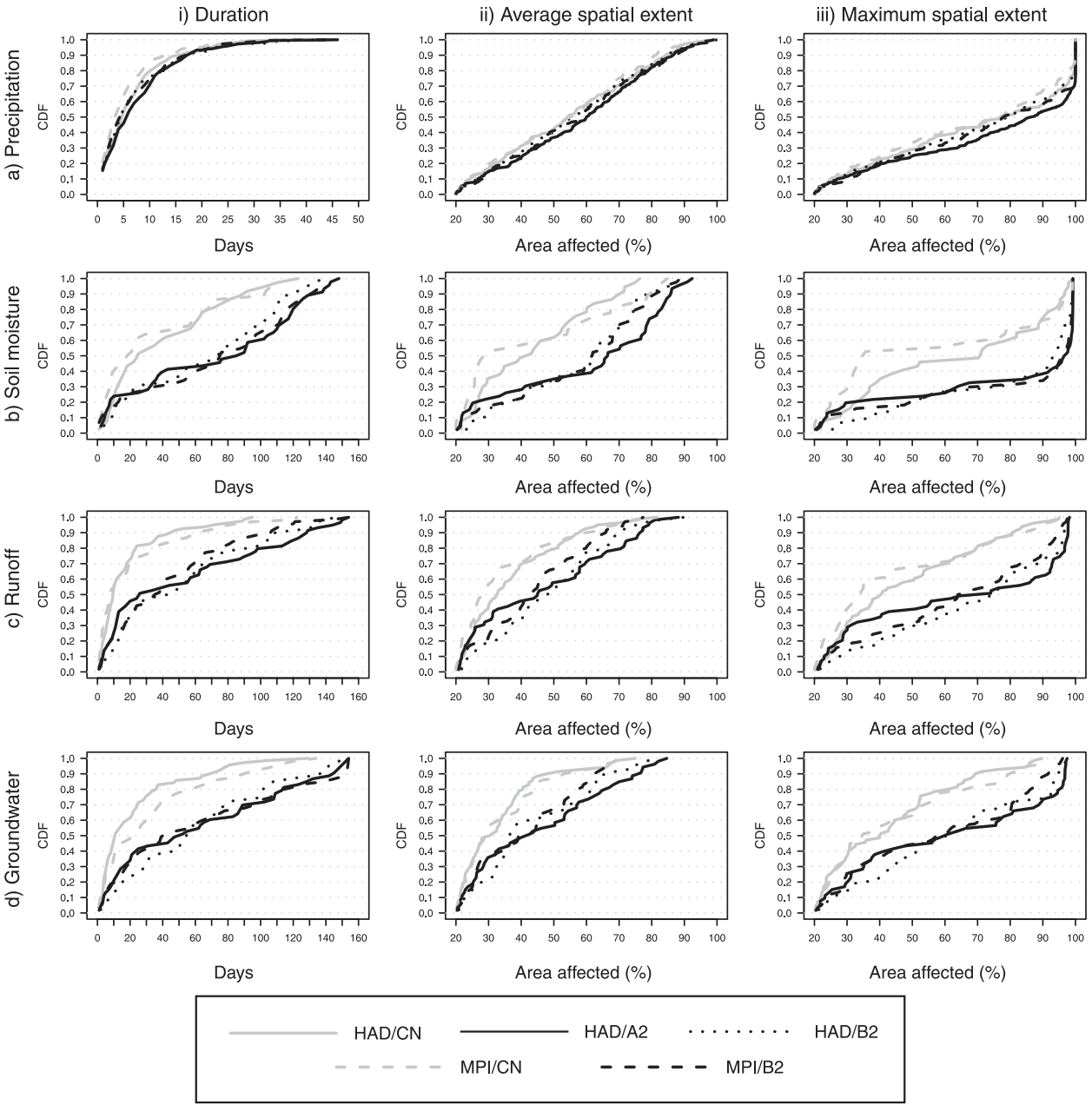

FIG. 6. The cumulative distribution function of drought duration, average, and maximum spatial extent for the Glomma River basin for (a) precipitation, (b) soil moisture, (c) runoff, and (d) groundwater. The solid and dashed gray lines represent HAD/CN and MPI/CN, respectively, for the control period (1961–90). The solid, dotted, and dashed black lines represent HAD/A2, HAD/B2, and MPI/B2 for the projection period (2071–2100).

changes in meteorological droughts in northern Norway, the increased summer temperatures will lead to significantly longer hydrological droughts (16–60 days) in many parts of this region (Figs. 4b–d). The effect is most prominent for the most severe hydrological droughts (Figs. 5b–d). However, in water-limited conditions like the considerable reduction of summer precipitation in southern Norway, the actual evapotranspiration is governed by the supply (precipitation) and not the demand. Consequently, the actual evapotranspiration decreases in southern Norway in a future climate (Fig. 2c); the longer hydrological droughts for this region are thus a result of reduced precipitation.

Figure 3 illustrates how different hydrological processes change the drought signal from short meteorological droughts (a few days) to longer droughts in soil moisture

(20–60 days), runoff (20–80 days), and groundwater (20–110 days). When the groundwater table is lowered, water is drained from the unsaturated zone. During episodes of infiltration, the soil moisture content rises above the hydrostatic equilibrium value to allow vertical flow, followed by a rise of the groundwater table and a new equilibrium state. As evapotranspiration draws water from the soil profile a soil moisture deficit relative to hydrostatic equilibrium develops. This deficit or demand on soil moisture must be satisfied before water is made available for percolation to the groundwater table and runoff. As a result, evapotranspiration occurs at the expense of runoff generation and groundwater recharge and a hydrological drought may develop (Nyberg 1995). In addition, basin properties, such as soil-water-retention characteristics and aquifer storage capacities, determine how fast runoff and groundwater respond to the lack of precipitation (Tallaksen and van Lanen 2004) and affect the development of a hydrological drought. The significant increase in changes in drought duration from meteorological droughts to hydrological droughts is observed for both average and maximum drought durations (Figs. 4 and 5).

b. Uncertainties

The simulation results presented here did not consider the effect of CO_2 on vegetation (i.e., the effect on stomatal conductance and the effect on leaf area index) or vegetation growth. The results of Betts et al. (2007) indicated that taking this effect into account would lead to decreased evapotranspiration and hence increased runoff, as compared to ignoring the effect. However, the results of Bounoua et al. (2010) suggested that when vegetation was allowed to increase its leaf density in response to CO_2 fertilization and climate, the associated increase in precipitation generated by the increase in CO_2 contributed primarily to increased evapotranspiration rather than surface runoff. These somewhat contradictory results may depend on model parameters; see, for example, discussion in Alkama et al. (2010). According to the results of Gerten et al. (2008), Alkama et al. (2010), and Bounoua et al. (2010), the effect of climate change largely drives the changes in evapotranspiration and runoff, and Alkama et al. (2010) quantified the climate change effect to account for 86% of the annual runoff increase during the twenty-first century. Hence, the results presented here should be valid, although including the effects of CO_2 on vegetation in the model simulations might yield slightly different results. The effects of CO_2 on vegetation in Norway are definitely interesting topics for further research.

The HBV model calculates potential evapotranspiration using a temperature index approach. This is a common parameterization procedure adopted in hydrological models (e.g., Xu and Singh 2001), but it may not be valid under changed climate conditions because transpiration from plants depends on several factors, such as wind, humidity, radiation, and ambient air CO_2 concentration. These may in turn affect the feedback between the land surface and the atmosphere. Though several studies suggest that estimates of potential evapotranspiration based on mean temperatures are incorrect in the context of water cycle changes (Sheffield and Wood 2007; Hobbins et al. 2008; Roderick et al. 2009; Milly and Dunne 2010), Beldring et al. (2006) showed that evapotranspiration changes from 1961–90 to 2071–2100 predicted by the HBV model using the temperature index approach do not differ significantly from latent heat flux changes predicted by the second version of the Rossby Center Atmospheric Model (RCA2) (Bringfelt et al. 2001) for Norway. The RCA2 model calculates latent heat flux using the land surface scheme of the Interaction Soil–Biosphere–Atmosphere model (Noilhan and Planton 1989). In Beldring et al. (2006), evapotranspiration was determined by two methods: 1) using the temperature index approach for both the control and projection periods and 2) modifying actual evapotranspiration derived from the HBV model for the control period in order to reproduce latent heat flux changes from the control to the projection period predicted by the RCA2 model. Based on the modeling results of Beldring et al. (2006) applying these two methods for determination of future evapotranspiration, hydrological drought characteristics for four catchments in southern, eastern, western, and northern Norway were compared. The results clearly showed that there were no statistical significant differences (t tests with 5% significance level) in derived average and maximum drought durations for runoff, soil moisture, or groundwater in the projection period. This shows that the results using the temperature index approach are not biased for Norway compared to the method applied in the atmospheric model, which includes a more comprehensive potential evapotranspiration calculation.

Because of the temperature increase in the projection period, increased ice melt contributes to a reduction in drought duration in the areas dominated by glaciers (blue areas in Figs. 4c,d and Figs. 5c,d). However, these results should be interpreted with care as neither glacier dynamics nor glacier volume and area are correctly described by the HBV model. Bergström et al. (2007) showed that all glaciers in the Nordic countries will reduce their volume and areal extent in this century, and some will even disappear.

In the future, higher temperatures will give an earlier snowmelt of the seasonal snowpack. Hence, the summer season (i.e., the period with reduced infiltration combined with higher evapotranspiration losses) is prolonged, increasing the potential for more persistent hydrological droughts. Increased temperatures will lead to an earlier

start and a later end of the summer season. An analysis of the temperature data in the projection period revealed an earlier season start of 10–15 days and a later ending of 20–30 days if an average daily temperature of 0°C was used as an indicator. In Fig. 3d this affects the estimation of groundwater drought duration. In the projection period, the maximum groundwater droughts will last for the whole summer season in as much as 20% of Norway. In these areas, the increase in maximum groundwater drought duration is probably underestimated. For runoff only a very small fraction of the country (5%) has a maximum drought duration of 154 days and the underestimation of increased drought duration can therefore be assumed to be smaller. In cases of soil moisture and precipitation droughts the effect of a prolonged summer season can be assumed to be limited.

Generally the downscaled control data reproduce the observed drought statistics for average drought duration well. Maximum drought durations for the hydrological variables were overestimated, and the results related to this characteristic should be treated with care. The results of Engen-Skaugen (2007) indicated that the adjustment method slightly overestimates whereas the RegCM grossly underestimates the number of dry days for most of Norway. The sequencing of wet days is not corrected by the method. Both factors probably contribute to the differences between observed and downscaled data when considering maximum drought duration. However, the direction of change is less subject to bias than the magnitude. Since this study focuses on the relative change, it is reasonable to conclude that maximum drought duration will also increase in the future. The adjustment of precipitation and temperature is treated separately, and gives no warranty that any possible cross-correlation structure of the observed precipitation and temperature fields is preserved. This may also lead to differences between observed and simulated drought characteristics. This illustrates that the correction of RegCM output is a topic for further research. The control period used here (1961–90) is the latest normal period and is commonly used in regional climate modeling studies [e.g., Prediction of Regional Scenarios and Uncertainties for Defining European Climate Change Risks and Effects (PRUDENCE); Christensen and Christensen 2007]. However, if another control period had been used in this study, it might give slightly different results, and hence represents another source of uncertainty.

The distribution of precipitation is positively skewed, and a threshold level based on the 80th percentile in the case of daily precipitation implies that only droughts of very short durations will be selected. This may partly explain why the differences in average meteorological droughts are small. A higher threshold could give a larger spatial variation in meteorological droughts. However, the same percentile was chosen as threshold for all the variables to simplify the comparisons of their drought characteristics.

The differences between HAD/B2 and MPI/B2 may be considered as model uncertainty and the differences between HAD/A2 and B2 as scenario uncertainty. Judging from the significant changes in drought characteristics, the model uncertainty is larger than the scenario uncertainty.

In regions with highly heterogeneous hydrological conditions, difficulties in defining a drought event that spans a large spatial extent makes event-based drought characteristics less applicable. Grid cell–based drought characteristics developed for this study are more useful and better suited to deal with such inherent heterogeneity. They are able to better describe the spatial variability and patterns (Figs. 4–5). At any given time, a map of the drought-stricken area can also be produced to illustrate the spatial coverage of the drought.

c. Comparison with previous studies

Lehner et al. (2006) examined the annual maximum drought deficit volume based on daily discharge data from the Water—Global Analysis and Prognosis (WaterGAP) hydrological model at a spatial resolution of $\sim 55 \times 55$ km^2. The projection period was the same as in this study, but the A1B scenario was used. The long term median (50th percentile) of monthly discharge was applied as the threshold level to select drought events. Their results indicate a reduction in 100-year streamflow droughts in Norway in the future. The significant increase in maximum summer drought duration shown in this study reflects the opposite. However, it should be noted that the results are not directly comparable. Their study did not take into account future changes in the interannual variability of temperature and precipitation, which might contribute to the opposite results. Further, although deficit volume and duration are highly correlated (Hisdal et al. 2001), different threshold levels, spatial resolutions, and modeling approaches can each result in different outcomes. This study focuses on summer droughts and used a partial duration series approach where all events below a threshold level were included. The drought events selected by Lehner et al. (2006) may include winter droughts since they did not make any seasonal differentiation in their study. In addition, fewer droughts are selected using the annual maximum approach. This could have rendered their analyses more susceptible to uncertainty errors, particularly as their model was not specifically calibrated for Norway. The method presented in this paper is therefore believed to be more robust with respect to detecting climate change impacts on drought.

Sheffield and Wood (2008) analyzed monthly soil moisture data from eight AOGCMs and three emission scenarios (B1, A1B, and B2) at a $2° \times 2°$ grid resolution. The 90th percentile was applied as the threshold level for drought selection, but they did not distinguish between summer and winter droughts. They found relatively small absolute changes in the frequency of short term (4–6 months) soil moisture droughts in northern Europe toward the end of the century but significant changes in areal extent. According to the projections presented in this paper, more frequent and considerably longer soil moisture droughts in large parts of the country can be expected. Differences in the findings can be expected because of differences in the spatial and temporal resolution, seasonal divisions, and the representation of hydrological processes within the AOGCMs and the HBV model. In addition, Sheffield and Wood (2008) presented a regional-average value for northern Europe. Norway was therefore not an explicit unit for analyses. However, the results of the present study confirm their findings regarding the spatial coverage of drought, which suggest that a much larger area of Norway will be affected by soil moisture droughts in the future.

Results from this study are generally consistent with the findings of Feyen and Dankers (2009). They used output from the HIRHAM RegCM based on the A2 scenario to drive the LISFLOOD hydrological model. Drought deficit volume and 7-day minimum flow were considered based on daily discharge data from a coarser resolution grid (5×5 km^2). The 80th percentile was applied as the threshold level. Their results suggest a 75% increase in flow deficit volume and a 20%–40% reduction in 7-day minimum flow in the nonfrost season in Norway in the 2071–2100 period. These changes are particularly prominent in southeastern Norway, including the Glomma River, but along the coast of western and northern Norway a slight reduction (10%–20%) of drought deficit volume is expected. However, Feyen and Dankers (2009) only presented results for the major rivers in Norway. They attributed all upstream catchment changes to individual river cells, which led to the loss of information about the spatial variation within a catchment. As a result, the method applied in this paper shows larger spatial variability than that of Feyen and Dankers (2009). This emphasizes the importance of analyzing data of sufficient temporal and spatial resolution for the scale of interest.

6. Conclusions

This study investigates the effect of climate change on meteorological and hydrological drought characteristics in Norway. Changes in both drought duration and spatial extent were examined. Grid cell–based drought duration characteristics were developed to study drought severity over heterogeneous regions. Results show that these characteristics are useful descriptors of drought when spatial variation at the regional scale is of interest.

Results also reveal that temperature changes are of major importance with respect to changes in hydrological drought characteristics in general. In some regions, even if the climate becomes wetter, and meteorological droughts do not change, hydrological summer droughts (soil moisture, runoff, and groundwater) are expected to become more severe. However, when the reduction of summer precipitation becomes considerable, the actual evapotranspiration decreases. The changes in drought characteristics in these areas are no longer only controlled by temperature, but also by the lack of precipitation.

The average area affected by hydrological droughts will increase substantially in the future whereas there will only be a minor increase for meteorological droughts. Generally, southernmost Norway will be the region hardest hit in terms of increasing average hydrological drought duration (31–60 days). Northernmost Norway will also experience longer droughts (16–30 days). The changes in maximum drought duration for both meteorological and hydrological droughts are much larger than changes in the average drought duration.

The drought characteristics derived by applying a minimum area criterion to drought events in the Glomma River basin indicate that future meteorological droughts in this region will not change significantly. However, hydrological droughts will affect a larger area, especially at their maximum spatial extent. Prolonged drought durations are also expected, which implies that the longest drought events will become even more persistent.

The largest changes in both drought duration and areal extent are found under the A2 higher emission scenario. Though the lower emission scenario (B2) generates smaller changes, they still represent a considerable increase in hydrological drought duration for a large part of Norway. This deserves attention by the authorities and stakeholders. Regional differences within projections also indicate that future changes are likely to be heterogeneous. This emphasizes the need for representative data of adequate resolution for use in drought studies. Data from regional climate and hydrological models are usually too coarse to capture the full extent of spatial variations within drought events.

Short duration meteorological droughts are modified by hydrological processes and basin properties, which can in turn generate significantly longer soil moisture, runoff, and groundwater droughts. Average drought durations increase from a few days for meteorological droughts to 20–120 days for groundwater droughts.

Evapotranspiration, which is an important mechanism for the feedback between the land surface and the

atmosphere, also affects drought development. This study has only considered the change in evapotranspiration induced by an increase in temperature. Further investigation of the effect of changes in other meteorological parameters on the evapotranspiration process is also required. Vegetation changes due to climate change have not been examined either. Such changes may affect evapotranspiration, soil moisture redistribution, and groundwater recharge. Further studies are therefore necessary to assess the influence of these other factors on future droughts.

Knowledge and understanding of droughts, their severities, and spatial extent are prerequisites for establishing appropriate drought preparedness plans. The high-resolution maps presented provide an efficient means of comparing future drought characteristics across space for different variables and projections. The maps make it easier to communicate the likely effects of climate change to a wider population. They are also useful for identifying the areas that require further and more detailed studies. The maps may also help water managers and stakeholders take more proactive action in response to the projected changes.

Acknowledgments. The authors thank Zelalem Mengistu and Jess Andersen (NVE) for their assistance with the visualization tool, Donna Wilson (NVE) for proofreading, Eirik J. Førland (met.no) for fruitful discussions, and three anonymous reviewers for their constructive comments and suggestions, which helped improve the manuscript. This work was partly supported by the European Union (FP6) funded Integrated Project called WATCH (Contract 036946).

REFERENCES

Alkama, R., M. Kageyama, and G. Ramstein, 2010: Relative contributions of climate change, stomatal closure, and leaf area index changes to 20th and 21st century runoff change: A modelling approach using the Organizing Carbon and Hydrology in Dynamic Ecosystems (ORCHIDEE) land surface model. *J. Geophys. Res.,* **115,** D17112, doi:10.1029/2009JD013408.

Beldring, S., L. A. Roald, and A. Voksø, 2002: Avrenningskart for Norge: Årsmiddelverdier for avrenning 1961-1990 (Map of annual runoff for Norway for the period 1961-1990). Norwegian Water Resources and Energy Directorate Doc. 2/2002, 49 pp. [Available online at http://www.nve.no/Global/Publikasjoner/Publikasjoner%202002/Dokument%202002/Trykkefil%202-02.pdf.]

——, K. Engeland, L. A. Roald, N. R. Sælthun, and A. Voksø, 2003: Estimation of parameters in a distributed precipitation-runoff model for Norway. *Hydrol. Earth Syst. Sci.,* **7,** 304–316.

——, L. A. Roald, T. Engen-Skaugen, and E. J. Førland, 2006: Climate change impacts on hydrological processes in Norway 2071-2100 based on RegClim HIRHAM and Rossby Centre RCAO regional climate model results. Norwegian Water Resources and Energy Directorate Rep. 5/2006, 59 pp. [Available online at http://www.nve.no/Global/Publikasjoner/Publikasjoner%202006/Report%202006/report5-06.pdf.]

Bergström, S., 1995: The HBV model. *Computer Models of Watershed Hydrology,* V.P. Singh, Ed., Water Resources Publications, 443–476.

——, and G. Sandberg, 1983: Simulation of groundwater response by conceptual models—Three case studies. *Nord. Hydrol.,* **14,** 71–84.

——, and Coauthors, 2007: Hydropower. *Impacts of Climate Change on Renewable Energy Sources: Their Role in the Nordic Energy System,* J. Fenger, Ed., Nordic Council of Ministers, 74–104. [Available online at http://www.nordicenergy.net/download.cfm?file=1120-C6036A69BE21CB660499B75718A3EF24.]

Betts, R. A., and Coauthors, 2007: Projected increase in continental runoff due to plant responses to increasing carbon dioxide. *Nature,* **448,** 1037–1041, doi:10.1038/nature06045.

Blenkinsop, S., and H. J. Fowler, 2007: Changes in drought frequency, severity and duration for the British Isles projected by the PRUDENCE regional climate models. *J. Hydrol.,* **342,** 50–71, doi:10.1016/j.jhydrol.2007.05.003.

Bounoua, L., F. G. Hall, P. J. Sellers, A. Kumar, G. J. Collatz, C. J. Tucker, and M. L. Imhoff, 2010: Quantifying the negative feedback of vegetation to greenhouse warming: A modeling approach. *Geophys. Res. Lett.,* **37,** L23701, doi:10.1029/2010GL045338.

Bringfelt, B., J. Räisänen, S. Gollvik, G. Lindström, P. Graham, and A. Ullerstig, 2001: The land surface treatment for the Rossby Centre Regional Atmospheric Climate Model—Version 2 (RCA2). Swedish Meteorological and Hydrological Institute Meteorology and Climatology Rep. RMK 98, 40 pp. [Available online at http://www.smhi.se/en/Publications/the-land-surface-treatment-for-the-rossby-centre-regional-atmospheric-climate-model-version-2-rca2-1.6663.]

Calanca, P., 2007: Climate change and drought occurrence in the Alpine region: How severe are becoming the extremes? *Global Planet. Change,* **57,** 151–160.

Christensen, J. H., and O. B. Christensen, 2007: A summary of the PRUDENCE model projection of changes in European climate by the end of this century. *Climatic Change,* **81,** 7–30, doi:10.1007/s10584-006-9210-7.

Colleuille, H., S. Beldring, Z. Mengistu, L. E. Haugen, T. Øverlie, J. Andersen, and W. K. Wong, 2008: Monitoring system for groundwater and soil water based on simulations and real-time observations: The Norwegian experience. *Proc. XXV Nordic Hydrological Conf.,* Reykjavik, Iceland, Nordic Hydrological Programme, 329–339. [Available online at http://www.nhf-hydrology.org/storage/conferences/nhc2008_vol2.pdf.]

Engen-Skaugen, T., 2007: Refinement of dynamically downscaled precipitation and temperature scenarios. *Climatic Change,* **84,** 365–382, doi:10.1007/s10584-007-9251-6.

Feyen, L., and R. Dankers, 2009: Impact of global warming on streamflow drought in Europe. *J. Geophys. Res.,* **114,** D17116, doi:10.1029/2008JD011438.

Fleig, A. K., L. M. Tallaksen, H. Hisdal, and S. Demuth, 2006: A global evaluation of streamflow drought characteristics. *Hydrol. Earth Syst. Sci.,* **10,** 535–552.

Frei, C., J. H. Christensen, M. Déqué, D. Jacob, R. G. Jones, and P. L. Vidale, 2003: Daily precipitation statistics in regional climate models: Evaluation and intercomparison for the European Alps. *J. Geophys. Res.,* **108,** 4124, doi:10.1029/2002JD002287.

Gerten, D., S. Rost, W. von Bloh, and W. Lucht, 2008: Causes of change in 20th century global river discharge. *Geophys. Res. Lett.,* **35,** L20405, doi:10.1029/2008GL035258.

Gordon, C., C. Cooper, C. A. Senior, H. Banks, J. M. Gregory, T. C. Johns, J. B. F. Mitchell, and R. A. Wood, 2000: The simulation

of SST, sea ice extents and ocean heat transport in a version of the Hadley Centre coupled model without flux adjustments. *Climate Dyn.,* **16,** 147–168.

Gottschalk, L., S. Beldring, K. Engeland, L. Tallaksen, N. R. Sælthun, S. Kolberg, and Y. Motovilov, 2001: Regional/macroscale hydrological modelling: A Scandinavian experience. *Hydrol. Sci. J.,* **46,** 963–982.

Hanssen-Bauer, I., and Coauthors, 2009: Climate in Norway 2100 (Klima i Norge 2100). Norsk Klimasenter Rep., 147 pp. [Available online at http://www.regjeringen.no/upload/MD/Kampanje/klimatilpasning/Bilder/NOU/klimatilpassing_endelig_lavoppl.pdf.]

Haugen, J. E., and T. Iversen, 2008: Response in extremes of daily precipitation and wind from a downscaled multi-model ensemble of anthropogenic global climate change scenarios. *Tellus,* **60A,** 411–426, doi:10.1111/j.1600-0870.2008.00315.x.

Hisdal, H., and L. M. Tallaksen, 2003: Estimation of regional meteorological and hydrological drought characteristics. *J. Hydrol.,* **281,** 230–247.

——, K. Stahl, L. M. Tallaksen, and S. Demuth, 2001: Have streamflow droughts in Europe become more severe or frequent? *Int. J. Climatol.,* **21,** 317–333.

——, L. M. Tallaksen, B. Clausen, E. Peters, and A. Gustard, 2004: Hydrological drought characteristics. *Hydrological Drought Processes and Estimation Methods for Streamflow and Groundwater,* L. M. Tallaksen and H. A. J. van Lanen, Eds., Developments in Water Sciences, Vol. 48, Elsevier Science, 139–198.

Hobbins, M. T., A. Dai, M. L. Roderick, and G. D. Farquhar, 2008: Revisiting the parameterization of potential evaporation as a driver of long-term water balance trends. *Geophys. Res. Lett.,* **35,** L12403, doi:10.1029/2008GL033840.

Larsen, R. J., and M. L. Marx, 1986: *An Introduction to Mathematical Statistics and Its Application*. 2nd ed. Prentice-Hall, 630 pp.

Lehner, B., P. Döll, J. Alcamo, T. Henrichs, and F. Kaspar, 2006: Estimating the impact of global change on flood and drought risks in Europe: A continental, integrated analysis. *Climatic Change,* **75,** 273–299, doi:10.1007/s10584-006-6338-4.

Lindström, G., B. Johansson, M. Persson, M. Gardelin, and S. Bergström, 1997: Development and test of the distributed HBV-96 model. *J. Hydrol.,* **201,** 272–288.

Ludwig, F., P. Kabat, H. van Schaik, and M. van der Valk, Eds., 2009: *Climate Change Adaptation in the Water Sector*. Earthscan, 274 pp.

Milly, P. C. D., and K. A. Dunne, 2010: On the hydrologic adjustment of climate-model projections: The potential pitfall of potential evapotranspiration. *Earth Interact.,* **15,** 1–14. [Available online at http://EarthInteractions.org.]

Nakićenović, N., and R. Swart, Eds., 2000: *Special Report on Emission Scenarios*. Cambridge University Press, 599 pp.

Noilhan, J., and S. Planton, 1989: A simple parameterization of land surface processes for meteorological models. *Mon. Wea. Rev.,* **117,** 536–549.

Nyberg, L., 1995: Water flow path interactions with soil hydraulic properties in till soil at Gårdsjön, Sweden. *J. Hydrol.,* **170,** 255–275.

Roderick, M. L., M. T. Hobbins, and G. D. Farquhar, 2009: Pan Evaporation Trends and the Terrestrial Water Balance II. Energy Balance and Interpretation. *Geogr. Compass,* **3,** 761–780, doi:10.1111/j.1749-8198.2008.00214.x.

Roeckner, E., L. Bengtsson, J. Feichter, J. Lelieveld, and H. Rodhe, 1999: Transient climate change simulations with a coupled atmosphere–ocean GCM including the tropospheric sulfur cycle. *J. Climate,* **12,** 3004–3032.

Sheffield, J., and E. F. Wood, 2007: Characteristics of global and regional drought, 1950–2000: Analysis of soil moisture data from off-line simulation of the terrestrial hydrologic cycle. *J. Geophys. Res.,* **112,** D17115, doi:10.1029/2006JD008288.

——, and ——, 2008: Projected changes in drought occurrence under future global warming from multi-model, multi-scenario, IPCC AR4 simulations. *Climate Dyn.,* **31,** 79–105, doi:10.1007/s00382-007-0340-z.

Solomon, S., D. Qin, M. Manning, M. Marquis, K. Averyt, M. M. B. Tignor, H. L. Miller Jr., and Z. Chen, Eds., 2007: *Climate Change 2007: The Physical Science Basis*. Cambridge University Press, 996 pp.

Tallaksen, L. M., and H. A. J. van Lanen, Eds., 2004: *Hydrological Drought—Processes and Estimation Methods for Streamflow and Groundwater*. Developments in Water Sciences, Vol. 48, Elsevier Science, 579 pp.

——, H. Hisdal, and H. A. J. van Lanen, 2009: Space–time modelling of catchment scale dought characteristics. *J. Hydrol.,* **375,** 363–372, doi:10.1016/j.jhydrol.2009.06.032.

Tveito, O. E., I. Bjørdal, A. O. Skjelvåg, and B. Aune, 2005: A GIS-based agro-ecological decision system based on gridded climatology. *Meteor. Appl.,* **12,** 57–68.

Vehviläinen, B., and Y. Motovilov, 1989: Simulation of soil frost depth and effect on runoff. *Nord. Hydrol.,* **20,** 9–24.

Wilson, D., H. Hisdal, and D. Lawrence, 2010: Has streamflow changed in the Nordic countries? – Recent trends and comparisons to hydrological projections. *J. Hydrol.,* **394,** 334–346, doi:10.1016/j.jhydrol.2010.09.010.

Xu, C.-Y., and V. P. Singh, 2001: Evaluation and generalization of temperature-based methods for calculating evaporation. *Hydrol. Processes,* **15,** 305–319.